

Electronic Supplementary Information (ESI)

Synergistic Solar-Powered Water-Electricity Generation Using a 3D-Printed Heatsink-like Device

Na Li,^{‡a,b} Jintao He,^{‡a,b} Jingjing Li,^a Zhaojun Li,^c Petri Murto,^{d,e} Zhihang Wang,^{*,f,g} & Xiaofeng Xu^{*,a}

^a College of Materials Science and Engineering, Ocean University of China, Qingdao 266404, China.

^b School of Rehabilitation Sciences and Engineering, University of Health and Rehabilitation Sciences, Qingdao 266113, China.

^c Solid State Physics Division, Department of Materials Science and Engineering, Uppsala University, Lägerhyddsvägen 1, 751 03 Uppsala, Sweden.

^d Yusuf Hamied Department of Chemistry, University of Cambridge, Cambridge, CB2 1EW, United Kingdom.

^e Department of Chemistry and Materials Science, Aalto University, Kemistintie 1, 02150 Espoo, Finland.

^f Department of Materials Science and Metallurgy, University of Cambridge, Cambridge CB3 0FS, United Kingdom.

^g School of Engineering, College of Science and Engineering, University of Derby, Markeaton Street, Derby DE22 3AW, United Kingdom.

* Corresponding authors: X. Xu, email: xuxiaofeng@ouc.edu.cn

Z. Wang, email: z.wang@derby.ac.uk

‡ These authors contributed equally to this work.

Table of Contents

1. Materials	S3
2. Instruments and methods	S3
3. FTIR characterization	S4
4. Effective evaporation areas.....	S4
5. Thermal conductivity measurements	S5
6. Energy loss and gain.....	S6
7. Water evaporation measurements at dark.....	S7
8. Water evaporation of SGs in harsh water conditions	S8
9. Salt resistance characterization	S8
10. Temperature of SGs under 1 sun	S9
11. Temperature of SGs under different solar irradiations	S10
12. I_{sc} of SGs under different solar irradiations	S10
13. Summary of thermoelectricity generation	S11
14. Summary of water-energy cogeneration.....	S12
15. References.....	S13

1. Materials

Bacterial cellulose nanofibers (BC) were purchased from Guilin Qihong Tech. Co., Ltd. $\text{FeCl}_3 \cdot 6\text{H}_2\text{O}$ and pyrrole were purchased from Shanghai Macklin Biochemical Co., Ltd, China. Glutaraldehyde (GA, crosslinker, 50 wt% in H_2O) and PEG-20000 were purchased from Sinopharm Chemical Reagent Co., Ltd, China. A commercial TEG ($3 \times 3 \text{ cm}^2$) was purchased from Guangzhou Sirui Electronic Technology Co., Ltd, China.

2. Instruments and methods

The absorption spectra were obtained from a UV–Vis–NIR spectrometer (LAMBDA 1050+, PerkinElmer) with an integrating sphere. The absorbance at each wavelength is defined by $1 - T - R$, where T and R are the corresponding transmittance and reflectance, respectively. The surface wettability of aerogels was evaluated by an optical contact angle meter (CA, JC2000DM, POWEREACH) combined with a camera. The morphologies and elemental mapping were characterized by a scanning electron microscope (VEGA3, TESCAN) in combination with energy dispersive X-ray spectrometry. The open-circuit voltage and power density were recorded and calculated using Keithley 2602B. The temperature was recorded by infrared thermal imager (Fotric 223s) and thermocouple (VC6801).

3. FTIR characterization

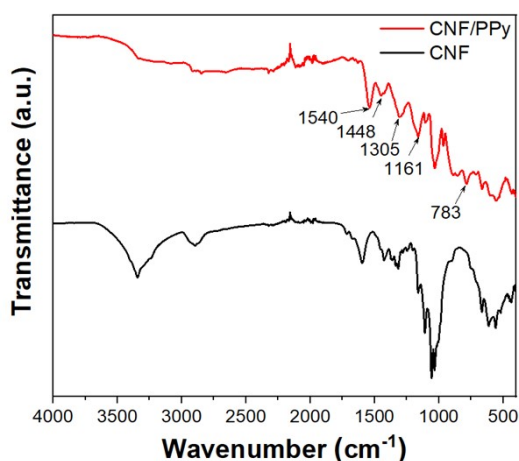


Figure S1. FTIR spectra of CNF and CNF/PPy aerogels.

4. Effective evaporation areas

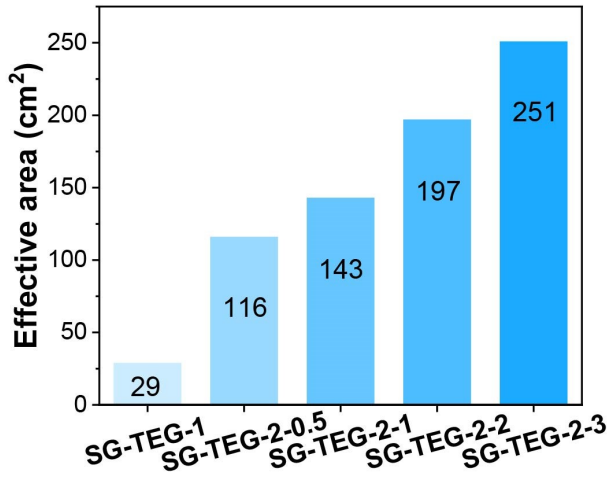


Figure S2. Effective evaporation areas of SGs.

5. Thermal conductivity measurements

The thermal conductivities of aerogels were measured via an IR imaging method¹. The samples were sandwiched between two 1.1 mm glasses. The sandwich structure was placed between copper plate heated by solar simulator and heat sink. The heat transfer rate (q) permeating the sample can be calculated using the Fourier Equation S1²,

$$q = -k_1 \frac{T_2 - T_1}{d_1} = -k \frac{T_3 - T_2}{d_2} \quad (\text{S1})$$

where k_l is the thermal conductivity of glass ($1.05 \text{ W m}^{-1}\text{K}^{-1}$). T_1 , T_2 , T_3 are the average temperatures at the interface of copper plate–top glass, top glass–sample, sample–bottom

glass, respectively. The thermal conductivities of samples (k) can be calculated by Equation S1 based on IR images.

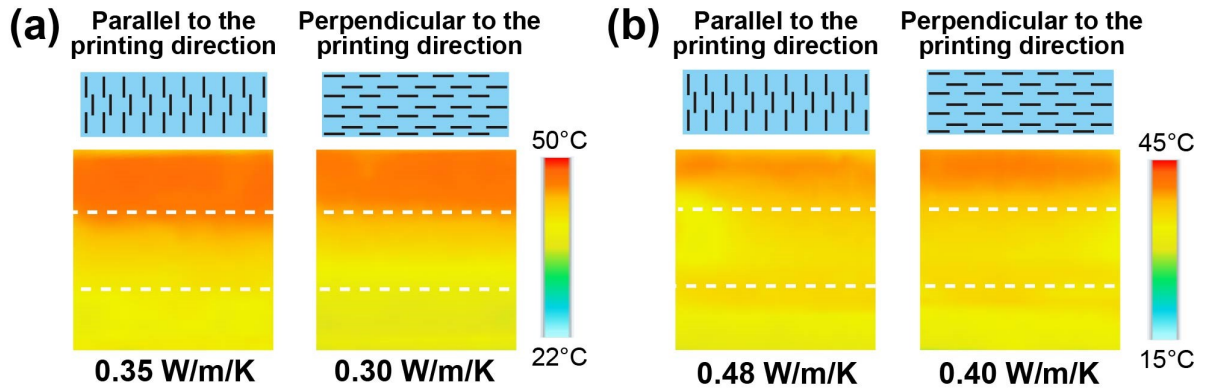


Figure S3. Thermal conductivities of aerogels in (a) dry and (b) wet state.

6. Energy loss and gain

a) Radiation loss:

The radiation loss was analyzed by Stefan-Boltzmann Equation S2,

$$\Phi = \varepsilon A \sigma (T_1^4 - T_2^4) \quad (\text{S2})$$

Φ is heat flux (W), ε denotes emissivity (Supposing the evaporator has a maximum emissivity of 1), A is hot evaporation surface area, σ represents the Stefan-Boltzmann constant ($\sigma = 5.670373 \times 10^{-8} \text{ W m}^{-2} \text{ K}^{-4}$), T_1 is the average surface temperature of the solar absorber after stable steam generation under 1-sun illumination. T_2 is the ambient temperature around the

evaporator. Therefore, based on Equation S2, we can calculate that the radiation heat loss is 5.3% for SG-TEG-1, 9.7% for SG-TEG-2.

b) Conduction loss:

The heat loss of convection was analyzed according to the following Equation S3,

$$Q = Cm\Delta T \quad (S3)$$

Q denotes the heat energy, C is the specific heat capacity of pure water ($4.2 \text{ kJ } ^\circ\text{C}^{-1} \text{ kg}^{-1}$), m represents the weight of bulk water and ΔT is the increased temperature of the bulk water after stable steam generation. In our experimental, $m = 100 \text{ g}$, $\Delta T = 11 \text{ }^\circ\text{C}$ for SG-TEG-1, $\Delta T = 0 \text{ }^\circ\text{C}$ for SG-TEG-2. Therefore, based on Equation S3, we can calculate that the conduction heat loss is 13% for SG-TEG-1, 0% for SG-TEG-2.

c) Convection loss:

The convection loss was calculated by Newton's law of cooling S4,

$$Q = hA\Delta T \quad (S4)$$

Q is the heat energy, h denotes the convection heat transfer coefficient ($\sim 5 \text{ W m}^{-2} \text{ K}^{-1}$). A represents surface area. ΔT is difference between the ambient temperature around the evaporator and the surface temperature of the evaporator. Therefore, based on Equation S4, we can calculate that the convection heat loss is 4.0% for SG-TEG-1, 7.4% for SG-TEG-2.

d) Reflection loss:

The reflection loss is 4.0% for SG-TEG-1 and SG-TEG-2.

e) Energy harvest:

The average temperatures of the side surface of steam generators were lower than room temperature, so energy was harvested from the environment through radiation and convection. Based on Equation S2 and S4, A is area of cold evaporation surface, we can calculate that the energy harvest of SG-TEG-1 and SG-TEG-2 are 0% and 52.6%.

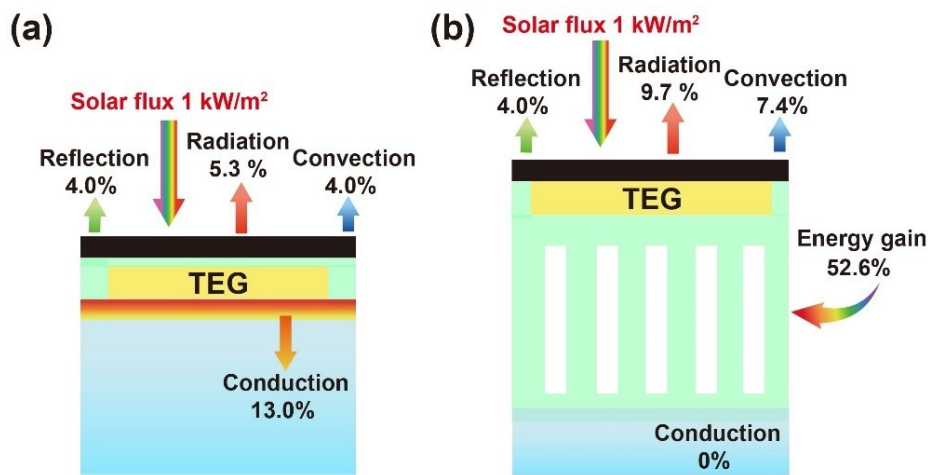


Figure S4. Schematic illustration of solar energy balance and energy transfer pathways of (a) SG-TEG-1, (b) SG-TEG-2.

7. Water evaporation measurements at dark

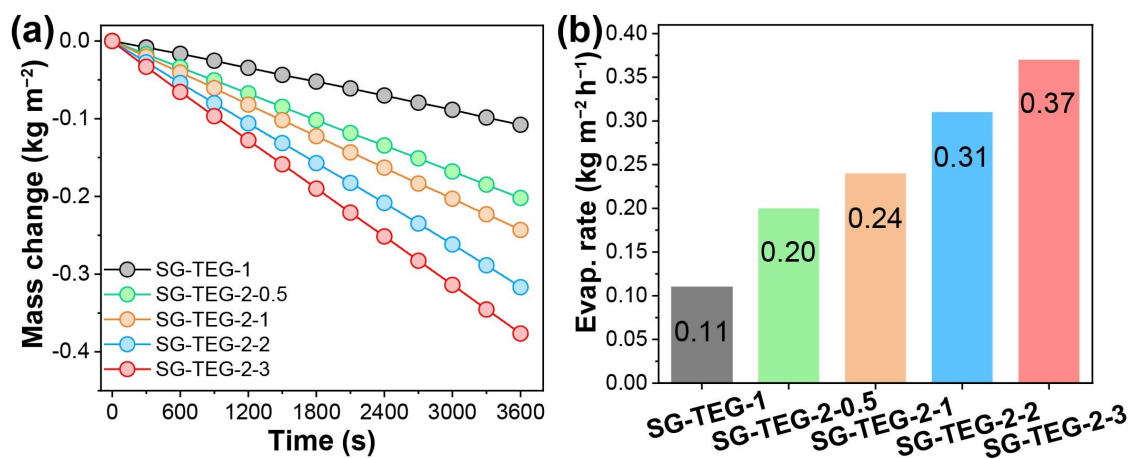


Figure S5. (a) Mass changes and (b) corresponding evaporation rates of SGs at dark.

8. Water evaporation of SGs in harsh water conditions

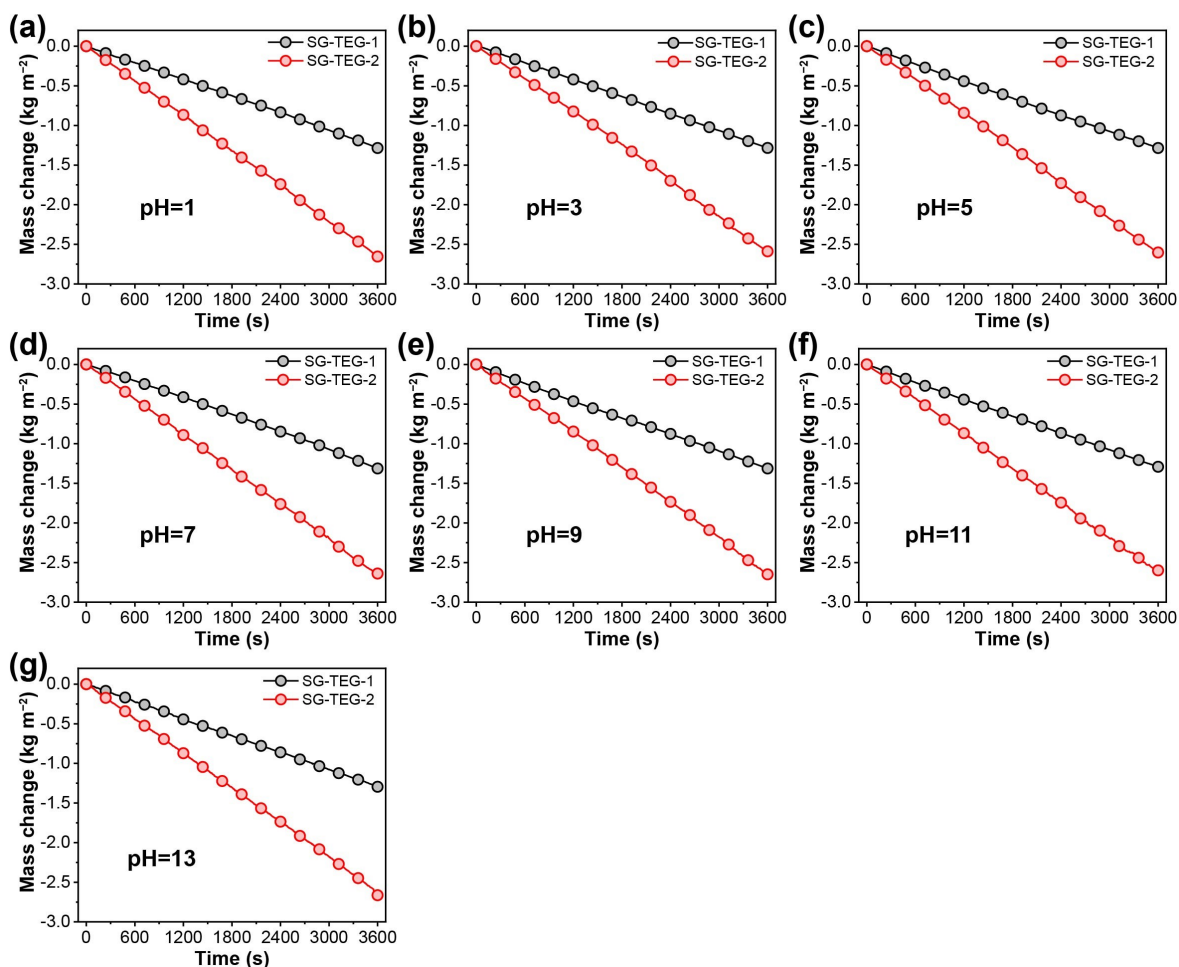


Figure S6. Mass changes of water over 1 h in different water conditions.

9. Salt resistance characterization

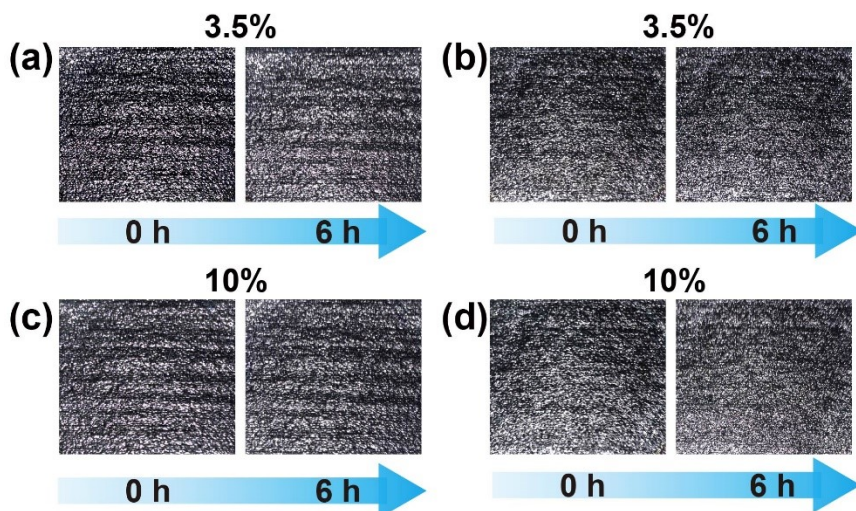


Figure S7. Digital photographs of salt sediment on (a, c) SG-TEG-1 and (b, d) SG-TEG-2.

10. Temperature of SGs under 1 sun

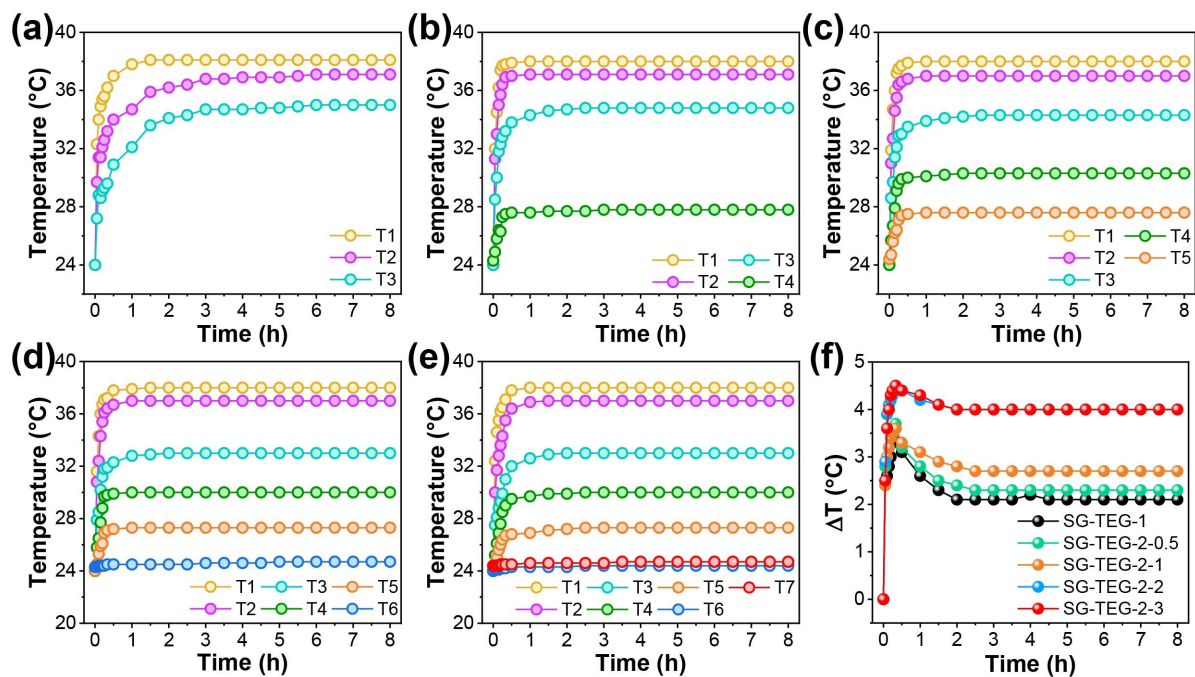


Figure S8. Temperature of (a) SG-TEG-1, (b) SG-TEG-1-0.5, (c) SG-TEG-1-1, (d) SG-TEG-1-2, (e) SG-TEG-1-3, and temperature differences of SGs under 1 sun.

11. Temperature of SGs under different solar irradiations

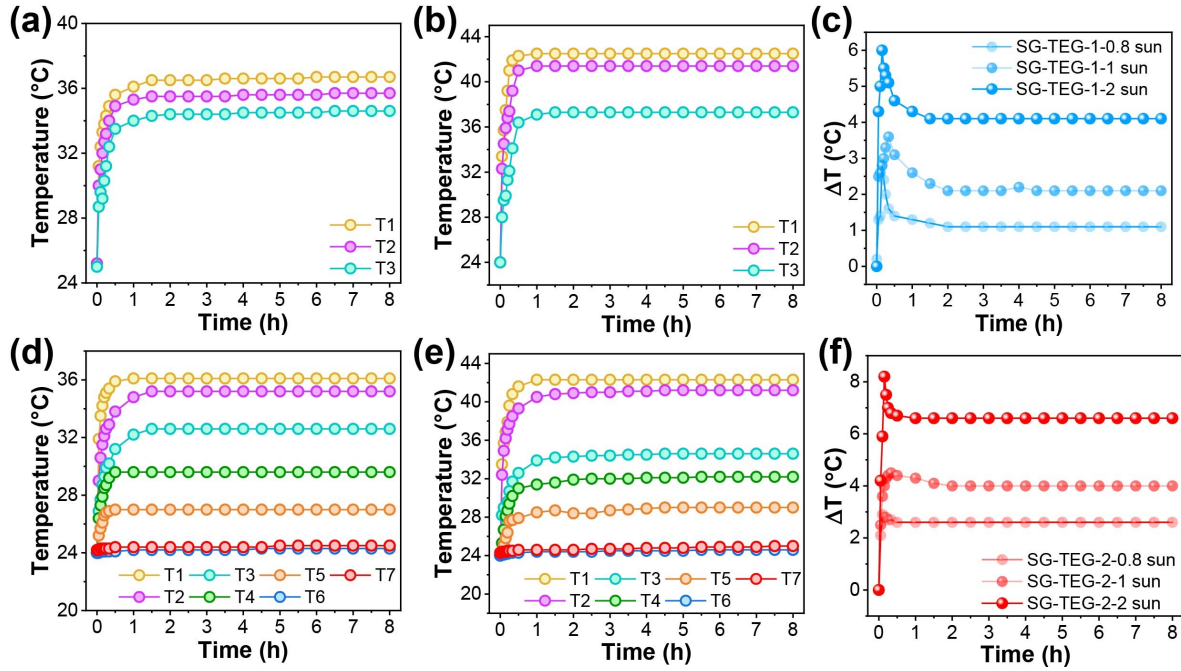


Figure S9. Temperature of SG-TEG-1 (a) under 0.8 sun and (b) under 2 sun, (c) temperature differences of SG-TEG-1 under different solar irradiations, temperature of SG-TEG-2-3 cm (d) under 0.8 sun and (e) under 2 sun, (f) temperature differences of SG-TEG-2-3 cm under different solar irradiations.

12. I_{sc} of SGs under different solar irradiations

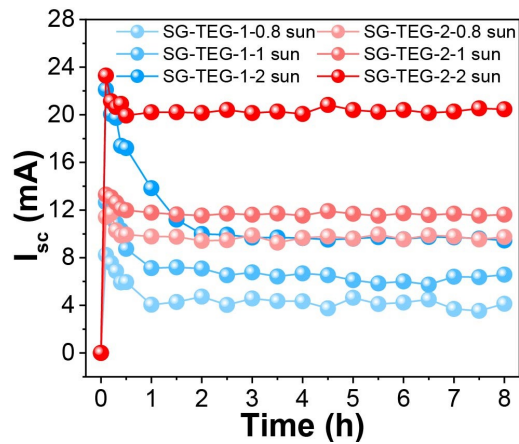


Figure S10. I_{sc} of SG-TEG-1 and SG-TEG-2 under different solar irradiations.

13. Summary of thermoelectricity generation

Table S1. Thermoelectricity generation of SG-TEG-1 and SG-TEG-2 under different solar irradiation.

Device	Solar irradiation (kW m ⁻²)	V_{oc} (mV)	I_{sc} (mA)	Maximum power density (W m ⁻²)
SG-TEG-1	0.8	13.5	4.2	0.016
SG-TEG-1	1	30	6.4	0.052
SG-TEG-1	2	62	9.6	0.17
SG-TEG-2	0.8	39.5	9.8	0.11
SG-TEG-2	1	60	11.5	0.19
SG-TEG-2	2	99.5	20.4	0.56

14. Summary of water-energy cogeneration

Table S2. Summary of water-energy cogeneration in recent reports.

Ref.	Evaporation rate ($\text{kg m}^{-2} \text{h}^{-1}$)	V_{oc} (mV)	I_{sc} (mA)	Time (min)	Light intensity (kW m^{-2})
3	0.83	35.73	-	5	1
4	1.35	40	9.75	90	1
5	1.37	50	11	30	1
6	1.45	76	7.8	60	1
7	1.65	12.5	-	30	1
8	1.70	75	12	10	1
9	0.89	43	-	5	1
10	1.39	19.76	-	8	1
11	1.29	59	9.5	30	1
12	1.39	60	26	60	1
13	1.40	23.5	2.5	7	1
14	1.21	45	9	15	1
15	0.98	55	-	5	1
16	1.02	51.3	13.8	10	1
17	1.26	40	9.57	90	1
18	2.30	89	-	60	1
19	1.00	51.9	-	3.3	1
20	1.98	27.3	1.38	5	1
21	3.54	52	-	60	1
This work	2.65	60	11.8	480	1

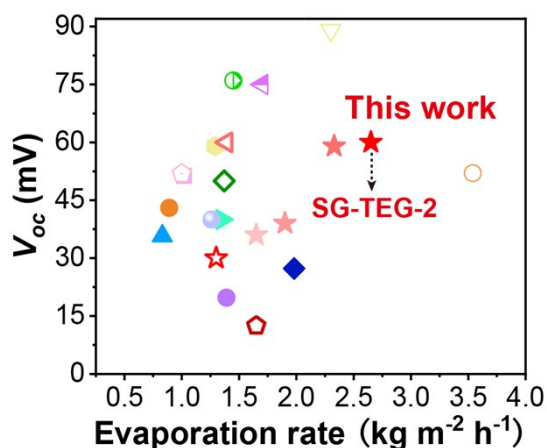


Figure S11. Summary of water-energy cogeneration in recent reports.

15. References

- 1 J. Wan, A. Fan, H. Yao and W. Liu. *Energy Convers. Manage.* 2015, **96**, 605.
- 2 H. Li, Y. He, Y. Hu and X. Wang. *Acs Appl. Mater. Interfaces* 2018, **10**, 9362-9368.
- 3 M. Shen, X. Zhao, L. Han, N. Jin, S. Liu, T. Jia, Z. Chen and X. Zhao. *Chem. Eur. J.* 2022, **28**, e202104137.
- 4 A. Ghaffar, Q. Imran, M. Hassan, M. Usman and M. U. Khan. *J. Environ. Chem. Eng.* 2022, **10**, 108424.
- 5 Z. Chen, X. Li, R. Liu, K. Ma, H. Sang, Y. Huang and C. Tang. *Ind. Eng. Chem. Res.* 2022, **61**, 16565-16576.
- 6 Y. Sun, Z. Zhao, G. Zhao, Y. Yang, X. Liu, L. Wang, D. Jia, X. Wang and J. Qiu. *J. Mater. Chem. A* 2022, **10**, 9184.
- 7 J. Jiang, H. Jiang, Y. Xu and L. Ai. *Desalination* 2022, **539**, 115977.
- 8 Z. Lin, T. Wu, Y. F. Feng, J. Shi, B. Zhou, C. Zhu, Y. Wang, R. Liang and M. Mizuno. *ACS Appl. Mater. Interfaces* 2022, **14**, 1034.
- 9 Y. Cui, J. Liu, Z. Li, M. Ji, M. Zhao, M. Shen, X. Han, T. Jia, C. Li and Y. Wang. *Adv. Funct. Mater.* 2021, **31**, 2106247.
- 10 X. Liu, D. D. Mishra, Y. Li, L. Gao, H. Peng, L. Zhang and C. Hu. *ACS Sustain. Chem. Eng.* 2021, **9**, 4571-4582.
- 11 H. Jiang, L. Ai, M. Chen and J. Jiang. *ACS Sustain. Chem. Eng.* 2020, **8**, 10833.
- 12 L. Zhu, T. Ding, M. Gao, C. K. N. Peh and G. W. Ho. *Adv. Energy Mater.* 2019, **9**, 1900250.
- 13 A. G. Saad, A. Gebreil, D. A. Kospa, S. A. El-Hakam and A. A. Ibrahim. *Desalination* 2022, **535**, 115824.
- 14 Y. Wu, Y. Li, Y. Long, Y. Xu, J. Yang, H. Zhu, T. Liu and G. Shi. *ACS Appl. Mater. Interfaces* 2022, **14**, 40437.
- 15 X. Han, Z. Wang, M. Shen, J. Liu, Y. Lei, Z. Li, T. Jia and Y. Wang. *J. Mater. Chem. A* 2021, **9**, 24452.
- 16 B. Jin, Y. Lu, X. Zhang, X. Zhang, D. Li, Q. Liu, B. Deng and H. Li. *Chem. Eng. J.* 2023, **469**, 143906.
- 17 A. Ghaffar, M. Usman, M. U. Khan and M. Hassan. *J. Clean. Prod.* 2024, **446**, 141374.
- 18 Q. Zhao, H. Wen, J. Wu, X. Wen, Z. Xu and J. Duan. *Desalination* 2024, **570**, 117064.
- 19 J. Li, L. Wang, C. Zhang, H. Wang, Y. Pan, S. Li, X. K. Chen, T. Jia and K. Wang. *Angew. Chem. Int. Ed.* 2024, **63**, e202402726.

- 20 A. G. Saad, S. A. El-Hakam, A. I. Ahmed, A. A. Ibrahim and A. Gebreil. *J. Water Process Eng.* 2024, **58**, 104840.
- 21 B. Nie, W. Zhang, X. Dou, Y. Meng, X. Zhao, Y.-C. Wu and H.-J. Li. *J. Mater. Chem. A* 2024, **12**, 293-302.